Accepted Manuscript

Knowledge representation using non-parametric Bayesian networks for tunneling risk analysis

Fan Wang , Heng Li , Chao Dong , Lieyun Ding

PII: S0951-8320(18)31571-0
DOI: https://doi.org/10.1016/j.ress.2019.106529
Article Number: 106529
Reference: RESS 106529

To appear in: *Reliability Engineering and System Safety*

Received date: 29 December 2018
Revised date: 22 April 2019
Accepted date: 31 May 2019

Please cite this article as: Fan Wang , Heng Li , Chao Dong , Lieyun Ding , Knowledge representation using non-parametric Bayesian networks for tunneling risk analysis, *Reliability Engineering and System Safety* (2019), doi: https://doi.org/10.1016/j.ress.2019.106529

Highlights

- A non-parametric Bayesian network is developed for tunneling risk analysis
- The model is quantified by marginal distributions and pair-wise linear correlations
- Expert opinions on distributions and correlations are elicited
- The model includes both continuous and discrete variables
- The model is validated by real documented accidents

Title page

Knowledge representation using non-parametric Bayesian networks for tunneling risk analysis

Fan Wang [a], Heng Li [a], Chao Dong [b,*], Lieyun Ding [b]

a Department of Building and Real Estate, The Hong Kong Polytechnic University, Kowloon, Hong Kong

b School of Civil Engineering and Mechanics, Huazhong University of Science and Technology, Wuhan, PR China

* corresponding author

Knowledge representation using non-parametric Bayesian networks for tunneling risk analysis

Abstract:

Knowledge capture and reuse are critical in the risk management of tunneling works. Bayesian networks (BNs) are promising for knowledge representation due to their ability to integrate domain knowledge, encode causal relationships, and update models when evidence is available. However, the model development based on classic BNs is challenging when expert opinions are solicited due to the discretization of variables and quantification of large conditional probability tables. This study applies non-parametric BNs, which only require the elicitation of the marginal distribution corresponding to each node and correlation coefficient associated with each edge, to develop a knowledge-based expert system for tunneling risk analysis. In particular, we propose to use the pair-wise Pearson's linear correlations to parameterize the model because the assessment is intuitive and experts in the engineering domain are more familiar and comfortable with this notion. However, when Spearman's rank correlation is given, the method can also be used by modification of the marginals. The method is illustrated with a tunnel case in the Wuhan metro project. The expert knowledge of risk assessment for common failures in shield tunneling is integrated and visualized. The developed model is validated by real documented accidents. Potential applications of the model are also explored, such as decision support for risk-based design.

Keywords: non-parametric Bayesian networks; structured expert judgment; expert system; risk analysis; tunneling

1. Introduction

Tunneling projects are prone to failures because of the limited information on ground conditions. In particular, the tunnels drilled in urban areas, such as for metro systems, impose great risks on the stakeholders as well as third party properties and persons. Failures in urban tunnel construction can cause damage to existing structures, disrupt the serviceability of utilities, or even incur injuries and deaths. In the past decade, the number of tunneling projects has increased rapidly as a result of underground space exploitation for sustainable economic development. Unfortunately, these tunnel works are accompanied by a number of accidents [1, 2]. Maintaining the safety during tunnel construction becomes a critical task for project managers.

The tunneling community has recognized the need for analyzing and managing the risks of tunnel works because large uncertainties (e.g., geotechnical and hydrological conditions, human and organizational factors) are involved [3, 4]. Risk management has proven to be an effective approach to the reduction of failures in tunneling projects [5]. Risk management practices require a great deal knowledge about the causes, conditions, and consequences of failure events. Evidence indicates that risk-related knowledge acquired from historical cases can potentially be useful in risk management for new projects [6-9]. Tunneling is a typical knowledge-intensive work. However, the relevant knowledge is often tacit and fragmented. As stated in previous studies, that knowledge resides mainly in the minds of people and is not shared among the stakeholders [10, 11]. Despite the efforts devoted to developing knowledge-based systems for risk analysis [12-14], the capture, representation, and reuse of risk-related knowledge remains a challenge because the details of accidents are often not disclosed [9]. Expert judgments are widely used in the absence of data to support the knowledge-based system development. Although judgments made by experts are usually uncertain, the information regarding variables are known, at least partially, from the personal experience of experts or inferred from other sources of knowledge [15]. Thus, the use of expert judgments can identify and deliver domain information to aid in decision-making [16]. Moreover, the structured elicitation and

aggregation of expert judgments are available in the literature [15, 17-20]. The reported protocols generally increase the reliability and robustness of the assessment obtained from experts.

The knowledge gained from the past needs to be properly visualized and integrated. As pointed out by Cárdenas et al. [21], construction risk-related knowledge can be transferred from project to project by means of causal models with probabilistic relationships. A few studies use event trees and fault trees to represent the knowledge about scenarios of tunnel construction failures [22, 23]. The occurrence probability of events is assessed from expert judgments, and the failure probability is calculated based on the dependence indicated by the graph. The combination of event and fault trees for the probabilistic risk assessment of tunnels is also proposed [24, 25]. However, these deductive and inductive methods are inflexible because the factors or events are sometimes partially related, and their relationships cannot be defined by simple logical functions. Recent studies have shown that the use of Bayesian networks (BNs) in conjunction with expert judgments is a promising approach in domain knowledge modeling [26-28]. A BN is a directed acyclic graph (DAG) consisting of a set of nodes and edges. The nodes represent the random variables, while the edges define the causal relationships among the random variables. The direct predecessors/successors of a node are termed parent/child nodes, and the nodes without parent nodes are called root nodes. The joint probability distribution is fully specified by the marginal distributions of the root nodes and conditional distributions corresponding to the child nodes. BNs have received increased attention because they enable a model to integrate domain knowledge, encode causal relationships, and update predictions as well as diagnoses when evidence is available [29].

BNs have been widely used in tunneling risk analysis. Sousa and Einstein [30] proposed two models based on BNs. The first model was developed for geology prediction, while the second model assisted the decision-making process on construction strategy. The risk during tunnel construction was minimized by taking into account both the cost of switching construction methods and the loss incurred by

tunnel failures. Špačková et al. [31, 32] applied a dynamic BN to assess the tunnel construction time. The models considered uncertainties in the excavation performance in each segment length and estimated the delays caused by extraordinary events such as human factors and tunnel collapses. Yu et al. [33] combined the construction simulation technique and a BN to calculate the occurrence probability of risk events under interrelated geological, design, construction, and management factors at each simulation step. Cárdenas et al. [9, 16, 21] established six models for major risks in tunnel works, including the excavation face instability, excessive volume loss, and leakage of the tunnel lining. The failure scenarios and probabilistic relationships were obtained based on extensive expert investigation. Because experts prefer to provide a linguistic expression while the computation of a BN requires the probability estimation of nodes, the fuzzy set theory is usually employed to bridge the gap. Zhang et al. used a fuzzy BN to assess the risk of tunnel leakage [34] and tunneling-induced damage to adjacent buildings [35], buried pipelines [36] and road surfaces [37]. These authors also used a BN to predict the ground settlement due to tunneling [38]. The other applications of fuzzy BNs for the probabilistic risk assessment of tunnel construction can be found in [39-41].

One commonality among the above BN models is that all the variables are discrete. In engineering practice, however, there are both discrete variables (such as the number of fatalities) and continuous variables (such as the support pressure). Working with continuous or hybrid (both continuous and discrete) variables has long been a problem in BNs. To be consistent with the classical BN quantification, each continuous variable has to be discretized into a finite number of non-overlapping intervals, which are later labeled as states of the corresponding node. In many cases, the determination of the bounds of these intervals seems subjective, and the discretization induces information loss. For example, it is difficult to discretize a variable whose value can be any real number. Several approaches, including dynamic discretization, are proposed to address the aforementioned problem [42, 43]; however, their implementation can be extremely challenging in practice [44]. Moreover, the discretization of continuous variables often leads to a large number of states for the

sake of reasonable approximation. As a result, the size of the conditional probability table can be very large, which means that the assessment burden is excessive and expert elicitation becomes infeasible.

To address these limitations, a non-parametric Bayesian network (NPBN) [44, 45] is adopted in this study to model the complex causal relationships in tunneling risk analysis. Compared to discrete BNs whose quantification relies on prior and conditional probability tables, the joint probability distribution of NPBNs is built on marginal distributions of the nodes and copulas [46] associated with the edges representing dependences. The quantification of NPBNs is thus simplified to the specification of a number of marginal distributions equal to the number of nodes and a number of copula parameters equal to the number of edges [44]. Moreover, the copulas allow the modeling of multivariate distributions in isolation of their marginal distributions. Thus, the discretization process is unnecessary.

The application of the NPBN method can be found in several different fields [44, 45, 47-50]. The information needed to quantify an NPBN can be estimated from data or elicited from experts. When expert opinions are solicited, the domain experts are usually queried regarding the conditional probability of a child node given its parent nodes [51]. This elicitation process, however, is unintuitive, particularly when the number of parent nodes is large. As argued by Clemen et al. [52, 53], the most accurate way to obtain a dependence structure underlying two variables from experts is simply to ask them about their correlation. Motivated by this observation, this study attempts to construct the NPBN by eliciting expert judgments on the marginal distributions and pair-wise correlations. Fig. 1 shows the procedures of the NPBN model development based on experts domain knowledge. After the determination of the network structure, the occurrence probabilities of nodes and correlations between dependent nodes are queried. The bivariate probability contour and scatter plot are used to visualize the dependence structure, while a bisection method is proposed to narrow the interval of estimates of correlations. Moreover, most dependencies in NPBN models are parameterized by Spearman's rank correlation. From the perspective of computation, the estimation of the copula parameter from Spearman's

rank correlation can be viewed as a special case of Pearson's linear correlation when both marginal distributions are uniform between 0 and 1. In engineering practice, however, the use of Pearson's linear correlation is ubiquitous. The invited experts are not comfortable with the notion of rank correlation. Therefore, we propose to use Pearson's linear correlation to quantify the dependence. The developed model is then used to assess the risk of accidents due to face instability, poor boring orientation, and excessive tail void ground loss, which are common failure modes in tunnels excavated using a tunnel boring machine (TBM).

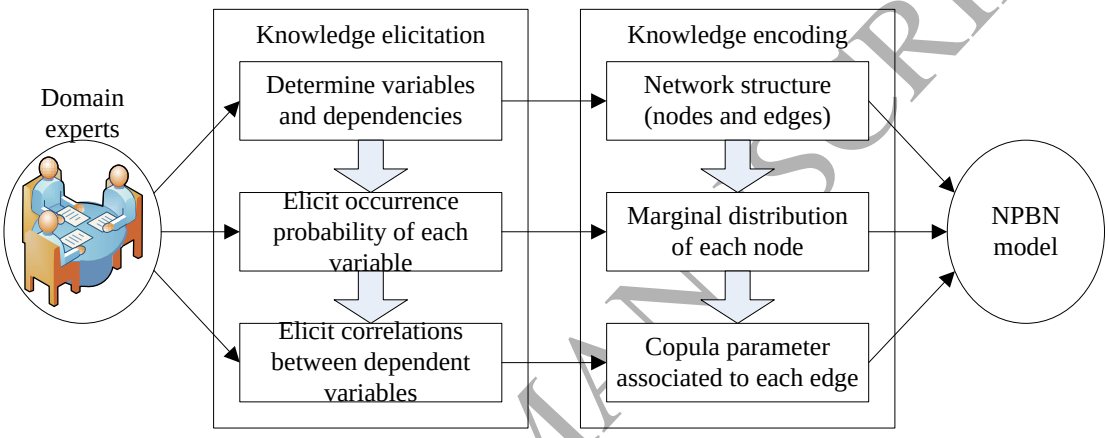

Fig. 1. Proposed knowledge representation method.

The remainder of this paper is organized as follows. Section 2 reviews the NPBN methodology. Section 3 presents the elicitation of marginal distributions and pair-wise linear correlations. Section 4 describes the quantification of NPBN models using elicited expert domain knowledge. Section 5 illustrates the method with a tunnel case in the Wuhan metro project. The developed model is validated using real documented accidents. The potential applications of the model are also discussed. Finally, the study is concluded in Section 6.

2. Non-parametric Bayesian networks

The calculation in a BN relies on the joint probability distribution of all the variables, which is factorized as:

$$f_{\mathbf{x}}(\mathbf{x}) = \prod_{i}^{n} f\left(x_i \mid x_{Pa(i)}\right) \tag{1}$$

where $\mathbf{x} = [x_1, \ldots, x_n]$ is an n-dimensional random vector whose elements are

represented by the nodes in the BN; $f(\mathbf{x})$ is the joint probability density function (PDF) of $\mathbf{x}$; $f\left(x_i \mid x_{Pa(i)}\right)$ denotes the conditional PDF of x_i corresponding to the *i*-th node given $x_{Pa(i)}$, where $Pa(i)=\left\{i_1,\ldots,i_{p(i)}\right\}$ indicates the parent nodes of the *i*-th node; and $f\left(x_i \mid x_{Pa(i)}\right)$ becomes the marginal PDF of x_i if $Pa(i)=\varnothing$.

The representation of the conditional PDF is critical to the factorization of the joint probability distribution. The copula theory [46] can be efficiently applied for this purpose. Considering two random variables x_i and x_j, the bivariate cumulative distribution function (CDF) can be expressed as:

$$F\left(x_i,x_j\right)=C\left(F_i\left(x_i\right),F_j\left(x_j\right);\theta_{i,j}\right)=C\left(u_i,u_j;\theta_{i,j}\right) \tag{2}$$

where $F_i\left(x_i\right)=u_i$ and $F_j\left(x_j\right)=u_j$ are the marginal CDFs of x_i and x_j, respectively; C is the copula function representing the underlying dependence structure; and $\theta_{i,j}$ is the copula parameter, which is related to dependence measures such as the correlation coefficient $r_{i,j}$ between x_i and x_j. Based on Eq. (2), the bivariate PDF of x_i and x_j can be written as:

$$f\left(x_i,x_j\right)=c\left(u_i,u_j;\theta_{i,j}\right)f_i\left(x_i\right)f_j\left(x_j\right) \tag{3}$$

where $c\left(u_i,u_j;\theta_{i,j}\right)=\dfrac{\partial C\left(u_i,u_j;\theta_{i,j}\right)}{\partial u_i \partial u_j}$ is the copula density function and $f_i\left(x_i\right)$ and $f_j\left(x_j\right)$ are the marginal PDFs of x_i and x_j, respectively. The conditional PDF of $f\left(x_j \mid x_i\right)$ can thus be written in terms of the copula as:

$$f\left(x_i \mid x_j\right)=\frac{f\left(x_i,x_j\right)}{f_j\left(x_j\right)}=c\left(u_i,u_j;\theta_{i,j}\right)f_i\left(x_i\right) \tag{4}$$

With the use of copulas, the modeling of the joint probability distribution can be achieved through the investigation of the marginal distributions and dependence structures separately. There are many copulas available in the literature [46]. In particular, the independence copula has the form $C\left(u_i,u_j;\theta_{i,j}\right)=u_i u_j$, which means

that x_i and x_j are independent. Moreover, a copula is said to have the zero independence property if uncorrelation entails independence, i.e., $r_{i,j}=0 \Leftrightarrow C\left(u_i,u_j;\theta_{i,j}\right)=u_iu_j$.

The above copula approach to modeling a bivariate joint probability distribution can be extended to multi-dimensions as long as the bivariate copula has a multivariate form. However, many multivariate copulas, such as the Archimedean copulas, are inflexible in representing multiple dependences. A more flexible way to construct a multi-dimensional joint probability distribution is thus proposed by using the pair-copula decomposition approach, or in particular, the vine-structured bivariate copula [54-56]. The conditional PDF in the form of $f\left(x_i \mid x_{Pa(i)}\right)$ can then be calculated recursively as:

$$f\left(x_i \mid x_{Pa(i)}\right)=c(F(x_i \mid x_{Pa(i)/i_k}),F(x_{i_k} \mid x_{Pa(i)/i_k});\theta_{i,i_k|Pa(i)/i_k})\,f(x_i \mid x_{Pa(i)/i_k}) \tag{5}$$

where $i_k \in Pa(i)$ is an arbitrarily selected element of $Pa(i)$, while $Pa(i)/i_k$ denotes the set $Pa(i)$ excluding the element i_k. The conditional CDF in the form of $F\left(x_i \mid x_{Pa(i)}\right)$ in Eq. (5) can be expressed as [57]:

$$\begin{aligned} F\left(x_i \mid x_{Pa(i)}\right) &= \frac{\partial C\left(F\left(x_i \mid x_{Pa(i)/i_k}\right),F\left(x_{i_k} \mid x_{Pa(i)/i_k}\right);\theta_{i,i_k|Pa(i)/i_k}\right)}{\partial F\left(x_{i_k} \mid x_{Pa(i)/i_k}\right)} \\ &= h\left(F\left(x_i \mid x_{Pa(i)/i_k}\right),F\left(x_{i_k} \mid x_{Pa(i)/i_k}\right);\theta_{i,i_k|Pa(i)/i_k}\right) \end{aligned} \tag{6}$$

where $h(\cdot)$ denotes the partial derivative of the copula function with respect to the second variable.

The remaining problem is the determination of a set of copula parameters. Suppose that for the *i*-th node, each edge $i_k \to i$ directed from its *k*-th parent node is associated with a correlation:

$$r_{i,i_k|i_1,\ldots,i_{k-1}}, k=1,\ldots,p(i) \tag{7}$$

The correlation is unconditional if $k=1$ and conditional if $k \geq 2$. Moreover,

the assignment is canceled if $Pa(i)=\varnothing$. Then, there is a one-to-one mapping relationship between $r_{i,i_k|i_1,\ldots,i_{k-1}}$ and $\theta_{i,i_k|i_1,\ldots,i_{k-1}}$, and the joint probability distribution of the variables in a BN is unique under a specific choice of a copula realizing all (conditional) dependence relationships while the (conditional) independence encoded in the graph of a BN is realized by the independence copula [44]. In particular, a copula that possesses the zero independence property can realize both the (conditional) dependence and independence and hence is widely used in practice.

For example, consider a BN with four nodes, as shown in Fig. 2. The joint probability distribution is factorized as follows:

$$f_{\mathbf{x}}(\mathbf{x})=f(x_1)\,f(x_2\mid x_1)\,f(x_3\mid x_1)\,f(x_4\mid x_2,x_3)$$

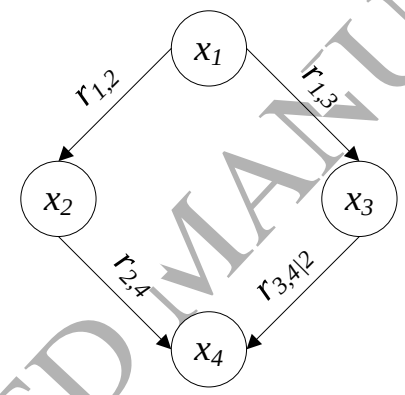

Fig. 2. A BN with four nodes.

Suppose the marginal PDF and CDF of each node are $f_i(x_i)$ and $u_i=F_i(x_i)$, $i=1,2,3,4$, respectively, and each edge is associated with a correlation measuring the dependence, i.e., $r_{1,2}$, $r_{1,3}$, $r_{2,4}$, and $r_{3,4|2}$. Then, the joint probability distribution can be written in terms of the copulas as:

$$f_{\mathbf{x}}(\mathbf{x})=c(u_1,u_2;\theta_{1,2})\,c(u_1,u_3;\theta_{1,3})\,c(u_2,u_4;\theta_{2,4})\times$$
$$c\left(h(u_4,u_2;\theta_{2,4}),h(u_3,u_2;\theta_{2,3});\theta_{3,4|2}\right)\prod_{i=1}^{4}f_i(x_i)$$

where $\theta_{1,2}$, $\theta_{1,3}$, $\theta_{2,4}$, and $\theta_{3,4|2}$ are determined based on $r_{1,2}$, $r_{1,3}$, $r_{2,4}$, and $r_{3,4|2}$, respectively. Note that $F(x_3\mid x_2)=h(u_3,u_2;\theta_{2,3})$ cannot be directly estimated

because $r_{2,3}$ is not given. However, the network structure implies that x_2 and x_3 are conditionally independent given x_1. Thus, we have:

$$
\begin{aligned}
F\left(x_3 \mid x_2\right) &= \int_{-\infty}^{+\infty}\int_{-\infty}^{x_3} \frac{f\left(y_1, x_2, y_3\right)}{f_2\left(x_2\right)} dy_3 dy_1 \\
&= \int_{-\infty}^{+\infty}\int_{-\infty}^{x_3} \frac{f_1\left(y_1\right) f\left(x_2 \mid y_1\right) f\left(y_3 \mid y_1\right)}{f_2\left(x_2\right)} dy_3 dy_1 \\
&= \int_{-\infty}^{+\infty}\int_{-\infty}^{x_3} c\left(F_2\left(x_2\right), F_1\left(y_1\right); \theta_{1,2}\right) f_1\left(y_1\right) f\left(y_3 \mid y_1\right) dy_3 dy_1 \\
&= \int_{-\infty}^{+\infty}\int_{-\infty}^{x_3} c\left(F_2\left(x_2\right), F_1\left(y_1\right); \theta_{1,2}\right) c\left(F_3\left(x_3\right), F_1\left(y_1\right); \theta_{1,3}\right) dF_3\left(y_3\right) dF_1\left(y_1\right) \\
&= \int_0^1 c\left(u_2, u_1; \theta_{1,2}\right) h\left(u_3, u_1; \theta_{1,3}\right) du_1
\end{aligned}
$$

The computation based on the specification of the marginal distribution of each node, the assignment of the (conditional) correlation to each edge, the implication of the (conditional) independence by the graph, and the use of copulas for multivariate distribution modeling is called the NPBN methodology [44, 45].

3. Elicitation of expert knowledge

The development of an NPBN model requires the quantification of univariate uncertainties and their dependences. When relevant data are scarce or absent, the only choice is to solicit expert opinions. Structured expert judgment has been widely used for deriving subjective probability distributions. A thorough review on the use of structured expert judgment for the elicitation of univariate and multivariate quantities can be found in the literature [20, 58]. This section describes the expert elicitation process for marginal distributions and pair-wise correlations. However, discrepant judgments are unavoidable because personal experience and knowledge vary from expert to expert. Therefore, it is necessary to carry out a discrepancy analysis and aggregate the divergent judgments.

3.1 Elicitation of expert opinions on the marginal distributions

Similar to the elicitation of node state probabilities in a discrete BN, the elicitation of marginal distribution in an NPBN is obtained by simply asking the expert about the probability of an event. However, a parametric distribution is fitted to

the elicited probabilities, which is achieved by determining the parameters of the distribution such that the fitting error is minimized. Commonly, a set of candidate parametric distributions is fitted and the distribution with the minimum approximation error is adopted. For continuous random variables, a set of continuous parametric distributions is examined. However, the support of a candidate continuous distribution should have practical sense for the modeled variable. For example, the excavation face pressure cannot be negative. Thus, only the distributions supported by positive real numbers, such as the Weibull distribution, should be investigated. For both lower and upper bounded variables, such as the geology prediction accuracy whose value is between 0 and 1, the beta distribution, for example, is more suitable. Similarly, the discrete parametric distributions are fitted for the discrete random variables unless the node is multi-state (in that case, the occurrence probabilities are directly assigned to a finite number of states as a probability mass function (PMF)). For example, the number of fatalities can be any integer equal to or larger than 0. However, it is not possible to ask an expert to give the whole PMF (i.e., assign a probability to each possible outcome) because the number of possible outcomes is infinite. Therefore, the fitting method based on a finite number of given probabilities is the only choice.

Specifically, let x be a random variable whose sample space is partitioned into q mutually exclusive subsets, $\Omega_i = \left\{ b_{l,i} < x \le b_{u,i} \right\}, i = 1, \ldots, q$, and the occurrence probability of the subset event is $\hat{p}_i$ given by an expert. The parameters of the parametric distribution model are then determined by minimizing the sum of squared differences with respect to the expert assessment:

$$\min_{\Theta} \sum_{i=1}^{q} \left(p_i - \hat{p}_i \right)^2 \tag{8}$$

with

$$\begin{cases} p_i = \int_{b_{l,i}}^{b_{u,i}} f\left(x;\Theta\right) dx & \text{if } x \text{ is continuous} \\ p_i = \sum_{b_{l,i} < b^{(m)} \le b_{u,i}} P\left(x = b^{(m)}; \Theta \right) & \text{if } x \text{ is discrete} \end{cases} \tag{9}$$

where $f(x;\Theta)$ is a univariate PDF and $P(x;\Theta)$ is a univariate PMF and Θ denotes the corresponding parameter of the PDF/PMF. The parameters $b^{(m)}, m=1,\ldots,M$ can be either real values or state indicators sorted in an ascending order indicating M possible outcomes of an event represented by x.

While the probability of a given subset event is queried in the above method as shown in Fig. 3, the knowledge can also be elicited by asking about the percentiles of the variable (see Fig. 3(a)). In other words, the expert is asked to provide the bounds corresponding to a cumulative probability [59]. However, the percentile method is not suitable for discrete variables because some percentiles do not exist. Moreover, in engineering practice, experts usually classify a variable into several categories. For example, the consequence of an accident may be serious, severe, and disastrous if the number of fatalities N_F is $N_F=1$, $1<N_F\leq 10$, and $N_F>10$, respectively [5]. This classification is either explicitly guided by the codes or implicitly performed according to the expert's own experience. Thus, it is more natural to ask the expert to define a set of subset events and then query their percentages.

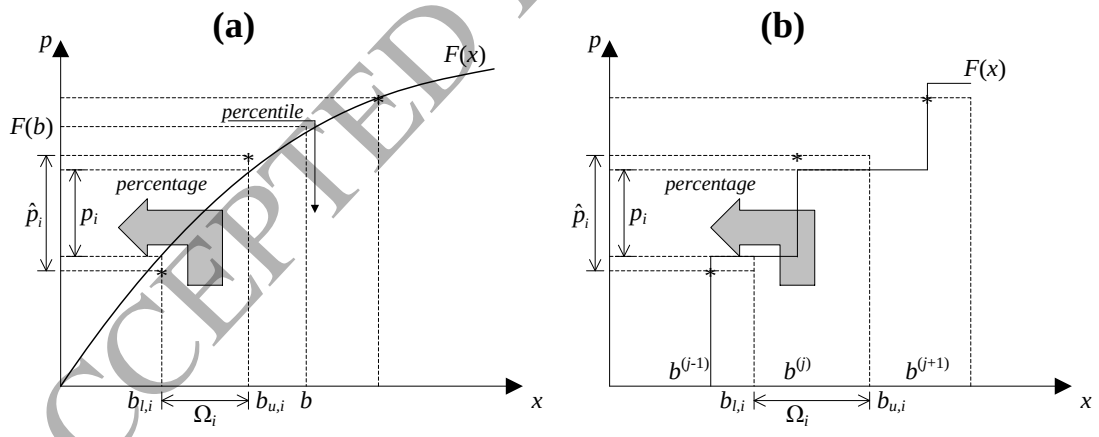

Fig. 3. Eliciting the probabilities for the parametric distribution fitting: (a) continuous case (b) discrete case.

3.2 Elicitation of expert opinions on the pair-wise correlations

When eliciting the dependence between random variables, a key problem is to determine the form of the dependence parameter. In general, the elicited forms can be grouped into two categories according to the assessment approach used [20]. The

probabilistic approach usually queries the conditional exceedance probabilities, concordance probabilities, or expected conditional percentiles. However, the probabilistic approach is recognized as cognitively difficult [53]. For example, it is not easy to assess a conditional probability if the dimension of the conditioning variables is high. In contrast, the statistical approach that queries the linear or rank correlation between two variables is deemed to be more accurate and imposes less assessment burden on the experts [53]. Although the use of Spearman's rank correlation is advocated [47, 51], most experts in tunneling domain work are more familiar with Pearson's linear correlation. Without proper training, the meaning of Spearman's rank correlation cannot be comprehended by the experts, and its arbitrary use can be misleading. Moreover, from a computational perspective, the estimation of the copula parameter from Spearman's rank correlation is a special case of the Pearson's linear correlation when both marginal distributions are uniform between 0 and 1. Thus, the dependence construction based on Pearson's linear correlation can be viewed as a generalization of previous methods. The following presents the relationship between Pearson's linear correlation and the copula parameter for different marginal cases.

(1) Both random variables are continuous

Let $r_{i,j}$ be the Pearson's linear correlation coefficient between x_i and x_j, whose marginal distributions are known with means μ_i and μ_j and standard deviations σ_i and σ_j, respectively. By definition, $r_{i,j}$ is expressed as:

$$r_{i,j} = \frac{E\left(x_i x_j\right) - \mu_i \mu_j}{\sigma_i \sigma_j} \tag{10}$$

where $E(\cdot)$ denotes the expectation. If both x_i and x_j are continuous, the copula parameter is determined by:

$$r_{i,j} = \frac{\iint_{\mathbb{R}^2} x_i x_j c\left(u_i, u_j; \theta\right) f_i\left(x_i\right) f_j\left(x_j\right) dx_i dx_j - \mu_i \mu_j}{\sigma_i \sigma_j} \tag{11}$$

Note that the Spearman's rank correlation coefficient is defined as the linear

correlation between the grades of x_i and x_j, i.e., the linear correlation between $u_i = F_i(x_i)$ and $u_j = F_j(x_j)$ where u_i and u_j are both uniformly distributed between 0 and 1. Thus, if we define $f_i(x_i) = f_j(x_j) = 1$, $\mu_i = \mu_j = \frac{1}{2}$, and $\sigma_i = \sigma_j = \sqrt{\frac{1}{12}}$, then Eq. (11) becomes the definition of the Spearman's rank correlation.

(2) Both random variables are discrete

If both x_i and x_j are discrete with M_i possible outcomes $x_i \in \left\{b_i^{(1)}, b_i^{(2)}, \ldots, b_i^{(M_i)}\right\}$ and M_j possible outcomes $x_j \in \left\{b_j^{(1)}, b_j^{(2)}, \ldots, b_j^{(M_j)}\right\}$, respectively, the integral in Eq. (11) becomes:

$$r_{i,j} = \frac{\sum_{m_i=1}^{M_i}\sum_{m_j=1}^{M_j} b_i^{(m_i)} b_i^{(m_j)} P\left(x_i = b_i^{(m_i)}, x_j = b_i^{(m_j)}\right) - \mu_i \mu_j}{\sigma_i \sigma_j} \tag{12}$$

with

$$\begin{aligned} P\left(x_i = b_i^{(m_i)}, x_j = b_j^{(m_j)}\right) = {} & C\left(u_i^{(m_i)}, u_j^{(m_j)}; \theta\right) - C\left(u_i^{(m_i-1)}, u_j^{(m_j)}; \theta\right) \\ & - C\left(u_i^{(m_i)}, u_j^{(m_j-1)}; \theta\right) + C\left(u_i^{(m_i-1)}, u_j^{(m_j-1)}; \theta\right) \end{aligned} \tag{13}$$

where $u^{(m)} = \sum_{s=1}^{m} P\left(x = b^{(s)}; \Theta\right)$ is the CDF of the discrete marginal distribution and $u^{(0)} = 0$. In particular, we have $P\left(x_i = b_i^{(1)}, x_j = b_j^{(1)}\right) = C\left(u_i^{(1)}, u_j^{(1)}; \theta\right)$ because the copulas are 'grounded'. Moreover, if x_i or x_j has an infinite number of possible outcomes (e.g., $P(x = b) = \frac{1}{2^b}$, $b = 1, 2, \ldots$), the right-hand side of Eq. (12) must be truncated at small probabilities for computational purposes.

(3) Mixed discrete-continuous random variables

Because $r_{i,j} = r_{j,i}$, without loss of generality, we assume that x_i is continuous and x_j is discrete and the bivariate distribution is decomposed as $f(x_i, x_j) = f(x_j \mid x_i) f_i(x_i)$. Then, Eq. (11) is re-written as:

$$r_{i,j} = \frac{\int_{\mathbb{R}} \sum_{m_j=1}^{M_j} x_i x_j P\left(x_j = b_j^{(m_j)} \mid x_i\right) f_i\left(x_i\right) dx_i - \mu_i \mu_j}{\sigma_i \sigma_j} \tag{14}$$

with

$$P\left(x_j = b_j^{(m_j)} \mid x_i\right) = h\left(u_j^{(m_j)}, u_i; \theta\right) - h\left(u_j^{(m_j-1)}, u_i; \theta\right) \tag{15}$$

When using Pearson's linear correlation, one major problem is that the attainable values of $r_{i,j}$ are usually strictly included in $[-1,1]$ due to the Fréchet-Hoeffding theorem. However, the mapping relationship between $r_{i,j}$ and θ is unique and all θ-values achieved through assigning a Spearman's rank correlation can also be realized using Pearson's linear correlation. It is the incompatibility between some values of linear correlations and marginal distributions that causes confusion. Another problem is that the elicited correlation matrix may not be positive definite. This problem can be addressed by setting constraints on each correlation to be assessed. The determination of the minimum and maximum of the attainable values of correlation will be presented in Section 4.

To facilitate the elicitation of the pair-wise correlation, we adapt the approach mentioned by Clemen and Reilly [52] that uses a scatterplot to visualize the strength of relationships between two random variables. As shown in Fig. 4, for continuous random variables, the scatterplot and the theoretical PDF isolines are presented for assessment. For the discrete case, the PMF is presented. For the mixed discrete-continuous case, the theoretical PDF/PMF of one variable conditioned on the other is presented. In addition, if the discrete variable has a large number of possible outcomes, the histogram is complemented; otherwise, the scatterplot is provided.

The bisection method is then adopted to obtain the exact value of the correlation coefficient. The elicitation process consists of the following steps:

Step 1: The expert is asked to identify whether the correlation is positive or negative;

Step 2: The upper and lower bounds of the attainable values are calculated (see Section 4) and several possible correlation values with equal intervals are selected.

The graphs corresponding to these correlations are delivered to the expert;

Step 3: If one graph that is believed to best represent the joint probability distribution is identified by the expert, the corresponding correlation coefficient is selected to quantify the dependence. Otherwise, the expert is asked to select two graphs corresponding to two correlation coefficients that represent the bounds of the belief of the expert and the process is continued to Step 4.

Step 4: The graph corresponding to the midpoint of the two correlation coefficients is plotted and Step 3 is repeated until the expert identifies the best graph or the expert cannot identify any difference between the new graphs. In the latter case, the midpoint of the last two correlation coefficients is selected to quantify the dependence.

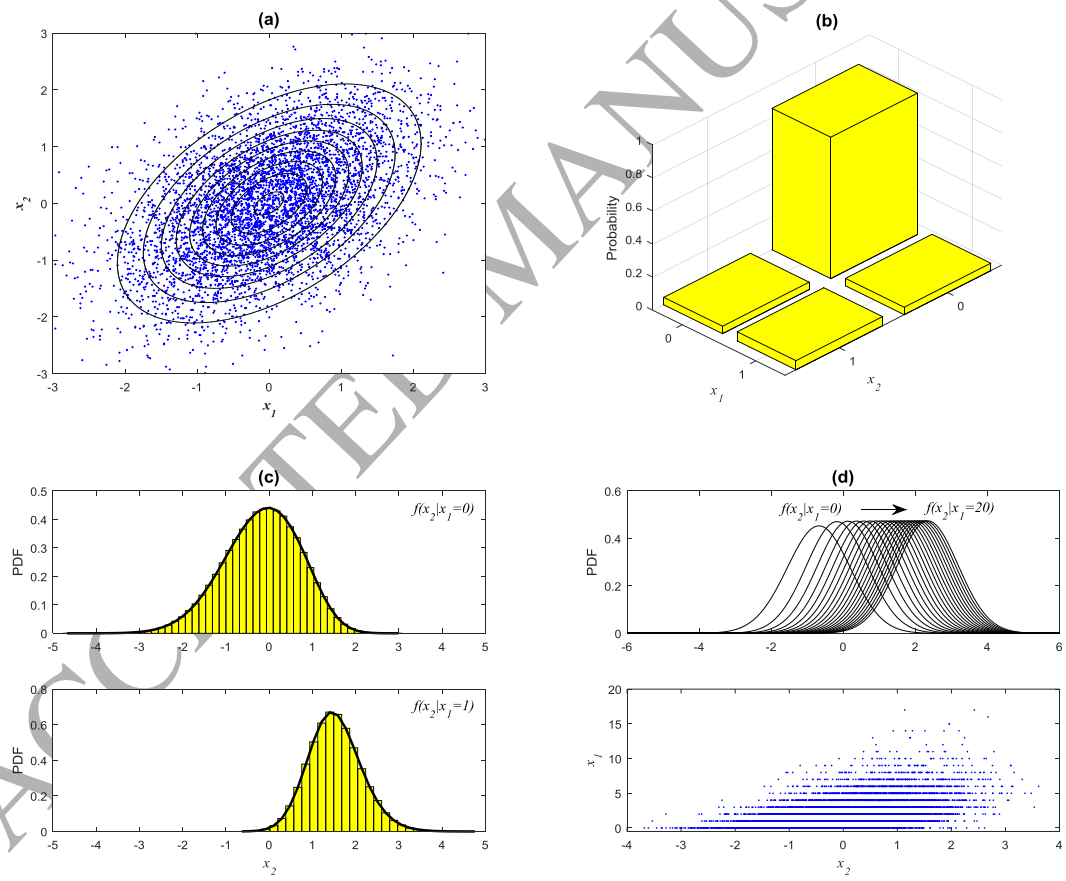

Fig. 4. Illustration of the visualized dependence between two random variables: (a) continuous case, both variables conform to standard normal distributions $x_1, x_2 \sim N(0,1)$; (b) discrete case, both variables conform to binomial distributions $x_1, x_2 \sim B(1,0.1)$; (c) mixed case, $x_1 \sim B(1,0.1)$

and $x_2 \sim N(0,1)$; (d) mixed case, the discrete variable conforms to a negative binomial distribution, $x_1 \sim NB(2,0.5)$, and $x_2 \sim N(0,1)$. The linear correlation coefficient is 0.5 in all cases, and a normal copula is assumed.

3.3 Discrepancy analysis and assessment aggregation

Discrepant expert assessments are unavoidable during the elicitation process and need to be combined. However, aggregating significantly divergent assessments may decrease the accuracy and credibility of the NPBN model. Thus, it is necessary to carry out a discrepancy analysis before aggregating divergent assessments. The aim of discrepancy analysis is to identify and eliminate outlier data, which originate from judgment-based biases [9]. Chauvenet's criterion is used here to identify the outlier data [60]. However, the identified outlier data are not removed; rather, a meeting is called to revisit those discrepant data. The experts are encouraged to justify their own assessments because each expert may have some evidence, derived from either through their own experience or acquired from other sources, that is not shared with the others. Then, a consensus is sought among the experts by discussion. This process of seeking a consensus is referred to as the behavioral aggregation method [20].

If no outlier data emerge, i.e., the data discrepancy is minor, the mathematical method, which uses a linear pooling model, is adopted for aggregation [20]. In this study, we use the equal weights decision maker that assigns an equal weight to each expert [61]. The performance-based decision maker, i.e., the weights are calibrated with seed variables, can be developed in future studies. Generally, a linear combination of the marginal probabilities is still a probability, while the weighted average of pair-wise correlation coefficients is still a correlation coefficient. Note that we only aggregate assessments on the pair-wise unconditional correlation coefficient corresponding to each edge, while the conditional independence encoded in the BN structure is not affected.

4. NPBN model parameterization using pair-wise correlations

When the marginal distribution of each node and the pair-wise correlation associated with each edge are determined, the joint probability distribution can be

constructed by selecting a copula and estimating its parameter. We use the multivariate normal copula for distribution modeling. The multivariate normal copula is defined as:

$$C(u_1,\ldots,u_n;\theta)=\Phi_n\left(\Phi^{-1}(u_1),\ldots,\Phi^{-1}(u_n);\boldsymbol{\rho}\right) \tag{16}$$

where Φ^{-1} is the inverse of a standard univariate normal CDF; Φ_n is the *n*-dimensional multivariate normal CDF with zero means and a fictive correlation matrix $\boldsymbol{\rho}$ as the copula parameters. We propose to use this copula because, first, it enables fast and exact inference [45]; second, it is equivalent to the vine-structured bivariate normal copula and thus is flexible [62]; and, third, the conditional correlations can be calculated analytically based on the unconditional pair-wise correlations, and thus, the transformation between the two is efficient [56].

There is a one-to-one mapping relationship between the correlation matrix of the random variables and the correlation matrix of the normal copula [52]. However, it must be ensured that the entry of $\boldsymbol{\rho}$ is attainable and the whole matrix is positive definite. Suppose that r_{i,i_k} is the unconditional correlation coefficient between the *i*-th node and its *k*-th parent node that needs to be assigned by an expert. Let $r_{i,i_k}=g_1\left(\rho_{i,i_k}\right)$ be the mapping relation defined as shown in Eq. (11), (12), or (14). Since $\left|r_{i,i_k}\right|\le\left|\rho_{i,i_k}\right|\le 1$ and r_{i,i_k} increases as ρ_{i,i_k} increases [63], the attainable values of r_{i,i_k} are bounded by (first constraint):

$$\begin{cases} r_{i,i_k}^{lb1}=g_1(-1) \\ r_{i,i_k}^{ub1}=g_1(1) \end{cases} \tag{17}$$

where r_{i,i_k}^{lb1} and r_{i,i_k}^{ub1} correspond to the copula version of the Fréchet-Hoeffding lower and upper bounds, respectively [46].

To guarantee that $\boldsymbol{\rho}$ is positive definite, we can use the constraints imposed on the conditional fictive correlation to derive the bounds of the entry of $\boldsymbol{\rho}$. Let $r_{i,i_k|i_1,\ldots,i_{k-1}}$ be the conditional correlation coefficient between the *i*-th node and its *k*-th

parent node as formulated in Eq. (7) and $r_{i,i_k|i_1,\ldots,i_{k-1}} = g_1\left(\rho_{i,i_k|i_1,\ldots,i_{k-1}}\right)$. The conditional fictive correlation coefficient can be calculated recursively by [56]:

$$\rho_{i,i_k|i_1,\ldots,i_{k-1}} = \frac{\rho_{i,i_k|i_1,\ldots,i_{k-2}} - \rho_{i,i_{k-1}|i_1,\ldots,i_{k-2}}\rho_{i_k,i_{k-1}|i_1,\ldots,i_{k-2}}}{\sqrt{\left(1-\rho^2_{i,i_{k-1}|i_1,\ldots,i_{k-2}}\right)\left(1-\rho^2_{i_k,i_{k-1}|i_1,\ldots,i_{k-2}}\right)}} \tag{18}$$

If the sub-matrix of $\boldsymbol{\rho}$ corresponding to the random vector $\left[\Phi^{-1}(u_i), \Phi^{-1}\left(u_{i_1}\right), \ldots, \Phi^{-1}\left(u_{i_k}\right)\right]$ is known except for the (i, i_k)-entry, $\rho_{i,i_k|i_1,\ldots,i_{k-1}}$ is dependent on ρ_{i,i_k} only. Let $\rho_{i,i_k|i_1,\ldots,i_{k-1}} = g_2\left(\rho_{i,i_k}\right)$ be the mapping relation. Because $r_{i,i_k|i_1,\ldots,i_{k-1}}$ is not specified and $\left|r_{i,i_k|i_1,\ldots,i_{k-1}}\right| \le \left|\rho_{i,i_k|i_1,\ldots,i_{k-1}}\right| \le 1$, the attainable values of r_{i,i_k} are bounded by (second constraint):

$$\begin{cases} r^{lb2}_{i,i_k} = g_1\left(g_2^{-1}(-1)\right) \\ r^{ub2}_{i,i_k} = g_1\left(g_2^{-1}(1)\right) \end{cases} \tag{19}$$

Thus, the value of the pair-wise correlation coefficient that the expert can assign to an edge is bounded by $\left[\max\left(r^{lb1}_{i,i_k}, r^{lb2}_{i,i_k}\right), \min\left(r^{ub1}_{i,i_k}, r^{ub2}_{i,i_k}\right)\right]$. If both marginals are uniform between 0 and 1, i.e., the Spearman's rank correlation is assigned, then $r^{lb1}_{i,i_k} = -1$ and $r^{ub1}_{i,i_k} = 1$. Thus, the Fréchet-Hoeffding lower and upper bounds do not affect the attainable value of r_{i,i_k} and r_{i,i_k} is bounded by $\left[r^{lb2}_{i,i_k}, r^{ub2}_{i,i_k}\right]$. In this case, the assignment is equivalent to the method proposed by Morales-Nápoles et al. [47] except that the pair-wise correlation, rather than a relative strength of correlation, is elicited.

Finally, the remaining entries of $\boldsymbol{\rho}$ are determined according to the conditional independence implied in the network structure. Let $x_{i_{nd}}$ be a non-descendent of x_i. Then, because the normal copula possesses the zero independence property, the fictive correlation between $x_{i_{nd}}$ and x_i is:

$$\rho_{i,i_{nd}|i_1,\ldots,i_{p(i)}} = g_2\left(\rho_{i,i_{nd}}\right) = 0 \tag{20}$$

For example, suppose the four random variables shown in Fig. 2 conform to a

standard normal distribution and the expert assigns $r_{2,4}$ and later $r_{3,4}$ (i.e., in original BN formulation, edge $2 \to 4$ is associated with $r_{2,4}$ and edge $3 \to 4$ is associated with $r_{3,4|2}$). In this case, for all edges, $r_{i,i_k}^{lb1} = -1$, $r_{i,i_k}^{ub1} = 1$ (the first constraint can be ignored), and $r_{i,i_k} = \rho_{i,i_k}$. Suppose the expert first assigns $\rho_{1,2} = 0.5$ and $\rho_{1,3} = 0.4$. Because x_2 and x_3 are conditionally independent given x_1, $\rho_{2,3}$ is determined by $\rho_{2,3|1} = 0$ using Eq. (18). Suppose that later the expert assigns $\rho_{2,4} = 0.6$. Then, the attainable values of $\rho_{3,4}$ can be estimated based on Eq. (19). Finally, suppose $\rho_{3,4} = 0.3$ is assigned by the expert, $\rho_{1,4}$ can then be determined based on the conditional independence between x_1 and x_4 given x_2 and x_3, i.e., $\rho_{1,4|2,3} = 0$. The process is summarized in Fig. 5.

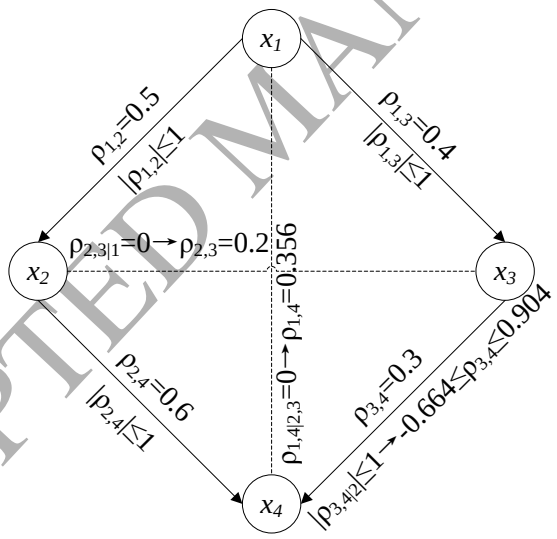

Fig. 5. Illustration of determining the normal copula parameters.

The establishment of the NPBN model is completed after the determination of the copula parameters. Then, the model can be updated when new observations are available. Suppose $\mathbf{x}$ is partitioned into $\mathbf{x} = \left[\mathbf{x}^{(1)}, \mathbf{x}^{(2)}\right]$ and mapped into $\mathbf{y} = \left[\mathbf{y}^{(1)}, \mathbf{y}^{(2)}\right]$ through the marginal transformation $y_i = \Phi^{-1}\left(F_i\left(x_i\right)\right)$. The corresponding fictive correlation matrices are partitioned accordingly into

$\boldsymbol{\rho} = \begin{bmatrix} \boldsymbol{\rho}^{(11)} & \boldsymbol{\rho}^{(12)} \\ \boldsymbol{\rho}^{(21)} & \boldsymbol{\rho}^{(22)} \end{bmatrix}$ where $\boldsymbol{\rho}^{(11)}$ and $\boldsymbol{\rho}^{(22)}$ are the correlation matrices of $\mathbf{y}^{(1)}$ and $\mathbf{y}^{(2)}$, respectively, and $\boldsymbol{\rho}^{(12)} = \boldsymbol{\rho}^{(21)}$ is the correlation matrix between $\mathbf{y}^{(1)}$ and $\mathbf{y}^{(2)}$. Then, the conditional distribution of $\mathbf{y}^{(1)}$ given observations of $\mathbf{y}^{(2)}$ is jointly normal with the following mean and variance:

$$\boldsymbol{\mu} = \boldsymbol{\rho}^{(12)} \left(\boldsymbol{\rho}^{(22)} \right)^{-1} \mathbf{y}^{(2)} \tag{21}$$

$$\mathbf{V} = \boldsymbol{\rho}^{(11)} - \boldsymbol{\rho}^{(12)} \left(\boldsymbol{\rho}^{(22)} \right)^{-1} \boldsymbol{\rho}^{(21)} \tag{22}$$

The simulation of $\mathbf{x}^{(1)}$ can thus be obtained using the inverse of the above marginal transformation from realizations of the conditional distribution of $\mathbf{y}^{(1)}$.

5. Case study

5.1 Overview of Wuhan metro project

The government of Wuhan had planned a metro project since the early 1990s. Up until October 2018, the Wuhan metro project has consisted of ten operational lines (Fig. 6). Meanwhile, there are more than 300 kilometers of metro tunnels that are under construction or to be constructed. Most tunnels were constructed using a TBM, either an earth pressure balance shield machine or a slurry shield machine.

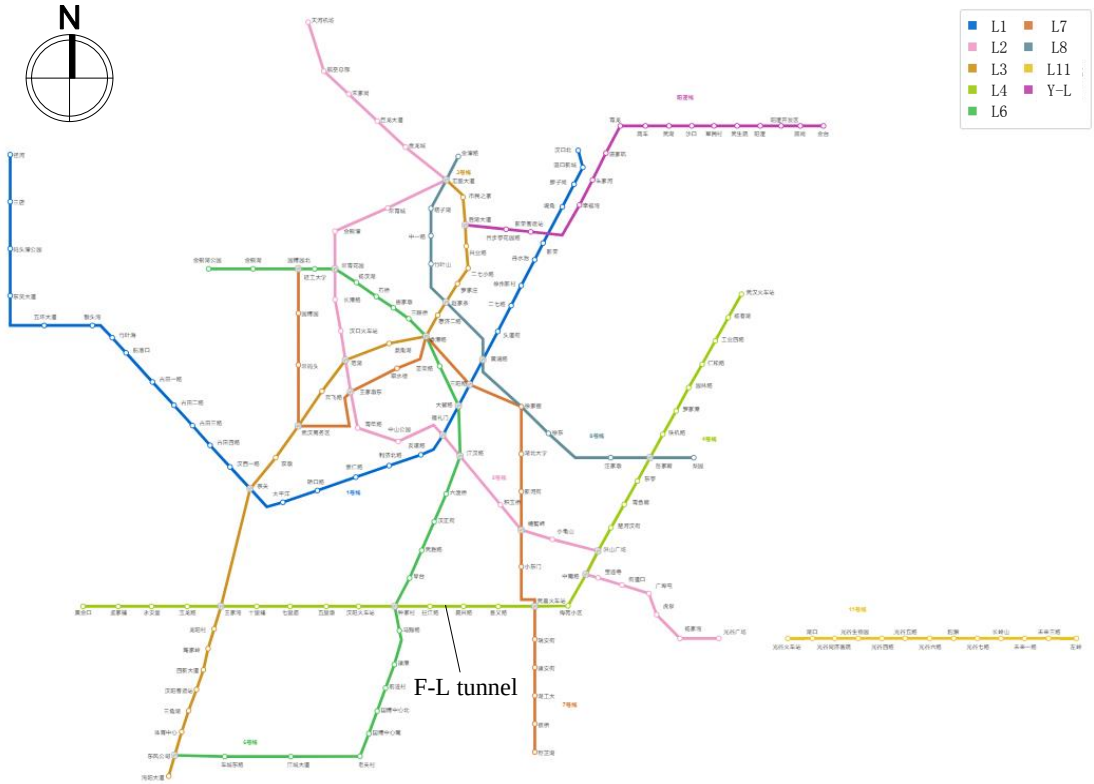

Fig. 6. Current Wuhan metro network.

The owner of the Wuhan metro project has employed a consultant company to perform a risk analysis since 2008. The main responsibility of the consultant company was to prioritize the risk of each tunnel under excavation and issue a risk report based on the instrumentation data and safety inspections on the tunnel structures, third party properties, and the environment, which are of major concern the owner, to support safety decisions. Although a large amount of data as well as inspection reports were generated during construction, the risk level of each construction site was largely determined based on expert's understanding of these extensive data and sets of evidence. Thus, it was necessary to establish a system that could visualize and reuse the knowledge of the experts in an explicit and efficient way.

5.2 NPBN model development

5.2.1 Network structure

The network structure was sketched based on literatures and domain knowledge. Four experts from the consultant company were then invited for possible corrections. All experts come from the consultant company and have at least five years of

experience in tunneling risk management of the Wuhan metro project. In particular, two experts have served the company since its foundation and have experienced the construction of multiple metro lines. Fig. 7 presents the final model structure for the tunneling risk analysis. The goal was to assess the potential human and economic loss per unit length excavated. Table 1 summarizes the variables considered in the model. There was one discrete node (X12), and the remaining nodes were continuous. The values of all variables were natural numbers. Discretization into several states, such as poor, fair, and good, was unnecessary. The symbol '+' or '-' associated with each edge indicated whether the dependency is positive or negative (an increase in the parent node would result in an increase or decrease in the child node).

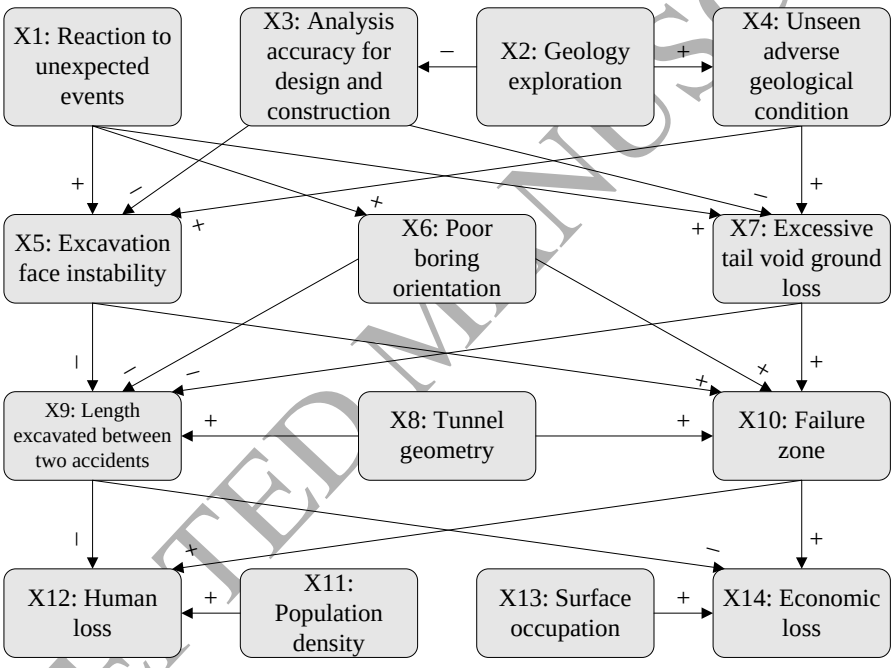

Fig. 7. NPBN model for the TBM tunneling risk analysis.

Table 1. Variables considered in the NPBN model

Node	Description
X1: Reaction to unexpected events	Average time elapsed between the occurrence of an unpredicted event and the control of the situation, i.e., the response time plus the time for counter-measures to take effect (unit: hours)
X2: Geology exploration	Average distance between two successive drilled boreholes along the tunnel axis for geological investigation (unit: m)
X3: Analysis accuracy of the design and construction	Percentage of the design and construction parameters that are set within reasonable ranges (%)
X4: Unseen adverse	Percentage of tunnels excavated within an adverse geology/hydrology

geological conditions	without proper pre-processing such as grouting or freezing (%)
X5: Excavation face instability	Average relative difference between the earth pressure and chamber pressure (%)
X6: Poor boring orientation	Tangent of the average pitching angle (dimensionless)
X7: Excessive tail void ground loss	Average ratio of the ground settlement due to the shield tail passing to the total ground settlement (%)
X8: Tunnel geometry	Average cover depth and diameter. Normalized as the cover-span ratio (dimensionless)
X9: Length excavated between two successive accidents	The node indicates the accident occurrence frequency (unit: km)
X10: Failure zone	The node indicates the area influenced by the accidents. It is defined as the ratio of the radius of the area to the tunnel cover depth (dimensionless)
X11: Population density	The node refers to the number of people exposed to risks. Defined as the average number of people per 100 square meters (unit: persons/100 m^2)
X12: Human loss	Fatalities per 10 kilometers excavated (unit: persons/10 km)
X13: Surface occupation	The node refers to the adjacent structures exposed to risks. Defined as the average floor ratio of the adjacent structures (dimensionless)
X14: Economic loss	Economic loss due to the tunneling-induced damage per 10 kilometers excavated. It is quantified in current Chinese Yuan (unit: CNY/10 km)

Generally, the causes of tunneling failure can be grouped into three factors: adverse geological conditions, inappropriate design and construction parameters, and poor management. The former two further depend on the degree of geology exploration, which is largely determined by the number of boreholes drilled along the tunnel alignment. The more boreholes are drilled, the higher the accuracy of the geology prediction. As a result, the ascertained adverse geologic conditions can be strengthened, and the tunnel is less likely excavated through an adverse geology. On the other hand, a detailed geological exploration can result in accurate modeling and analysis of the tunnels to be constructed, leading to appropriate design parameters and construction plans for the tunnel. However, geological exploration is costly and time consuming. Thus, it is usually not possible to drill boreholes at small intervals. Poor management is another main cause of failures. We used the summation of time in response to unexpected events and time spent on containing the situation to indicate the efficiency of construction management.

Three failure modes are commonly observed in shield tunneling due to the above

failure causes. Excavation face instability occurs when the pressure provided by the TBM is not in equilibrium with the earth pressure. A poor boring orientation means that the actual orientation of the shield is not maintained within the designed alignment. An excessive tail void ground loss implies that the shield tail grouting performance is not satisfactory; thus, the ground movement towards the circular tail void created between the shield skin and tunnel lining is not effectively prevented. All failure modes can induce large disturbances to the original ground stresses and may lead to accidents such as collapse or daylight collapse, excessive ground settlement, and damage to existing structures and facilities.

In practice, the excavation face pressure, the actual orientation, and the tail void ground loss cannot be balanced exactly, maintained accurately, or avoided completely all the time. However, large deviations in the face pressure, high pitching angles, and excessive tail void ground losses increase the likelihood and magnitude of accidents. The accident occurrences during tunneling can be modeled as a Poisson process [64]. We considered the total number of accidents that had occurred up to an excavated length. Thus, the length excavated between two successive accidents follows an exponential distribution. According to the experts, the average length excavated between two successive accidents is 3.7 km (i.e., the failure rate is approximately 0.27 km^{-1}), which is close to the results from other studies [31, 65]. The magnitude of an accident refers to the zone influenced by the accident. We used the radius of the influenced area at ground surface versus the tunnel depth (i.e., the tangent of the angle of the failure zone) to indicate the magnitude. In addition to the failure modes, the accident frequency and magnitude are also partially determined by the tunnel geometry, namely, the cover depth and tunnel shape. In the Wuhan metro project, the cross-sections of all tunnels constructed by TBM are circular. The cover-span ratio, defined as the ratio of the cover depth to the tunnel diameter, was used to indicate the tunnel geometry. Generally, shallow buried tunnels are more likely to experience accidents (e.g., daylight collapse) once a failure occurs, but the influenced zone tends to be smaller.

Finally, the consequences of the accidents, i.e., loss of human life and economic

loss, were assessed. Because metro lines are usually excavated in cities, in addition to the accident frequency and magnitude, the loss of human life and economic loss are related to the persons and properties involved in the accident, respectively. Accidents that occur in densely populated regions with high surface occupation levels are expected to have severe consequences.

There are more factors than summarized in Table 1 that can affect tunnel accidents, such as penetration rate, support pressure, and ground conditions. In this study, we kept the model small to make the knowledge elicitation process feasible. To this end, we assume that the failure modes arises from the unexpected ground conditions or incorrect parameter settings (rather than specific conditions or values). This simplification, however, does not reduce the value of the model for safety decisions. A more sophisticated model than the one presented in Fig. 7 can be developed in future studies, and the NPBN method, though illustrated with tunneling by TBM, can be extended to the risk analysis of tunnels constructed using the new Austrian tunneling method (NATM).

5.2.2 Elicitation of marginal distributions of nodes

The four experts were later invited to provide probability information. First, the information on the marginal probability distribution of each variable except node X9 (which was assumed to follow an exponential distribution and the failure rate was directly assessed as mentioned above) was elicited as shown in Section 3.1. Upper and lower bounded continuous distributions, such as the beta or truncated normal distribution, were examined for variables X3, X4, and X7 whose values are between 0 and 1, while several discrete distributions, such as the Poisson, binomial, or negative binomial distribution, were fitted to the discrete variable X12. A number of parametric continuous distributions, including the lognormal, gamma, Weibull, Gumbel minima, and Gumbel maxima distribution, were fitted to the remaining continuous variables with positive values. Since all considered variables are non-negative, distributions such as the normal distribution were not considered. For example, based on aggregated expert opinions, the percentages of reaction time (X1) are: a) <1h: 8%, b) 1-3h: 27%, c) 3-6h: 35% d) 6-12h: 26% e) >12h: 4%. Thus the cumulative

probabilities are $P(X_1<1)=0.08$, $P(X_1<3)=0.35$, $P(X_1<6)=0.70$, $P(X_1<12)=0.96$. Several parametric continuous CDFs are then fitted to these data. The Weibull distribution yields the minimum fitting error and thus is chosen to represent the node distribution. Fig. 8 illustrates the best fit marginal distributions based on the expert judgments on nodes X1 (half bounded continuous), X3 (both sides bounded continuous) and X12 (discrete).

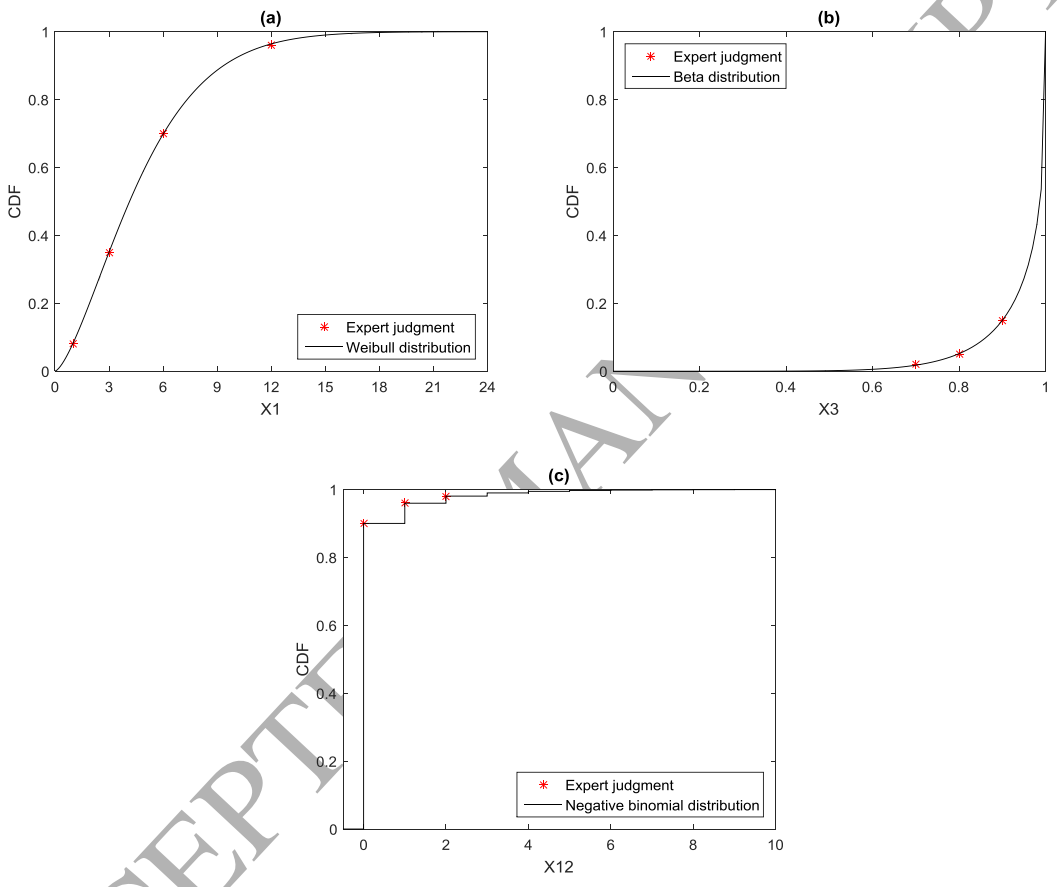

Fig. 8. Univariate distributions fitted based on the expert judgments: (a) continuous node X1 with positive values; (b) continuous node X3 with values bounded between 0 and 1; (c) discrete node X12.

5.2.3 Elicitation of correlations associated to edges

Second, the experts were queried on the pair-wise correlations associated with each edge. Graphs were used to visualize the joint probability distribution and aid the expert judgment, as shown in Section 3.2. The lower and upper bounds of each correlation were calculated before the elicitation. Table 2 lists the attainable values of each correlation. The graphs corresponding to several values with equal intervals were

then delivered to the experts, and they were asked to identify the one that best represents the relationship between two variables. For example, to elicit the correlation between X1 and X5, the lower and upper bounds [-0.661, 0.942] were first calculated. The experts were then queried whether the correlation is positive or negative. After the agreement that a positive correlation exists between X1 and X5, the scatterplots corresponding to $r_{1,5} = 0.1, 0.2, \ldots, 0.9$ were delivered to the experts. Two experts picked the picture with a correlation of 0.4. The other two experts believed that the correlation lies between 0.3 and 0.4 and between 0.4 and 0.5, respectively. The scatterplots corresponding to the midpoints of the above intervals were further delivered to the latter two experts, who accepted the refined values 0.35 and 0.45 as their respective opinions on the correlation. Finally, the average value 0.4 was adopted as the correlation between X1 and X5. During the elicitation process, no relationship was determined after more than three rounds of interviews, indicating that the experts were familiar and comfortable with the concept of Pearson's linear correlation. Fig. 9 shows a few graphs corresponding to the elicited correlations. The development of the NPBN model was completed once the correlations and marginals were elicited. Fig. 10 presents 1E5 realizations based on a model when no observation was available for conditioning, which is referred to as the unconditional case.

Table 2. Elicited pair-wise correlations based on expert judgments

Relationship	Correlation	Bounds	Relationship	Correlation	Bounds
X2-X3	-0.35	(-0.744, 0.855)	X8-X9	0.5	(-0.584, 0.677)
X2-X4	0.6	(-0.937, 0.852)	X5-X10	0.6	(-0.773, 0.884)
X1-X5	0.4	(-0.661, 0.942)	X6-X10	0.3	(-0.524, 0.840)
X3-X5	-0.6	(-0.847, 0.387)	X7-X10	0.5	(0.181, 0.975)
X4-X5	0.65	(-0.224, 0.698)	X8-X10	0.3	(-0.658, 0.680)
X1-X6	0.45	(-0.858, 0.999)	X9-X12	-0.175	(-0.248, 0.788)
X1-X7	0.5	(-0.951, 0.972)	X10-X12	0.2	(-0.319, 0.583)
X3-X7	-0.55	(-0.702, 0.671)	X11-X12	0.4	(-0.354, 0.489)
X4-X7	0.4	(-0.261, 0.649)	X9-X14	-0.075	(-0.108, 0.325)
X5-X9	-0.4	(-0.549, 0.987)	X10-X14	0.125	(-0.086, 0.208)
X6-X9	-0.15	(-0.682, 0.563)	X13-X14	0.1	(-0.095, 0.155)
X7-X9	-0.35	(-0.855, -0.098)			

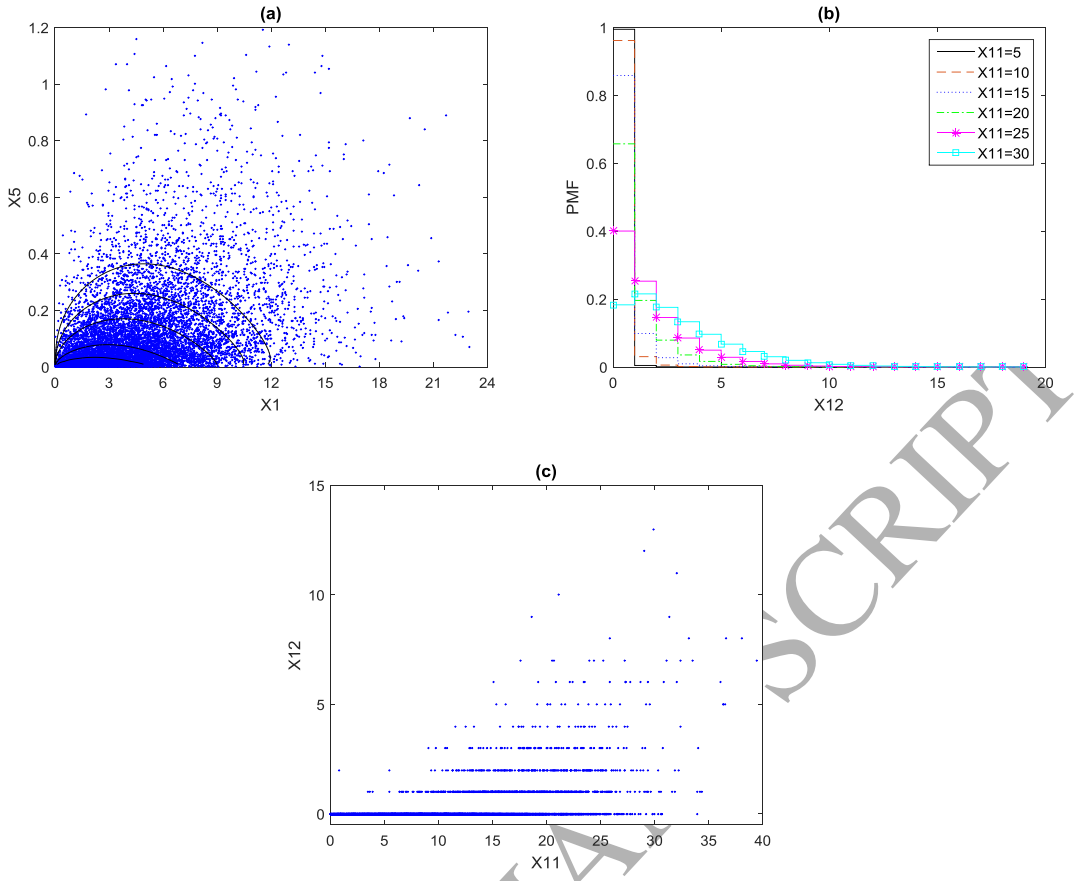

Fig. 9. Examples of the best dependence elicitation identified by experts: (a) scatterplot and PDF isolines of X1 and X5; (b) conditional PMF of X12 given X11; (c) scatterplot of X11 and X12.

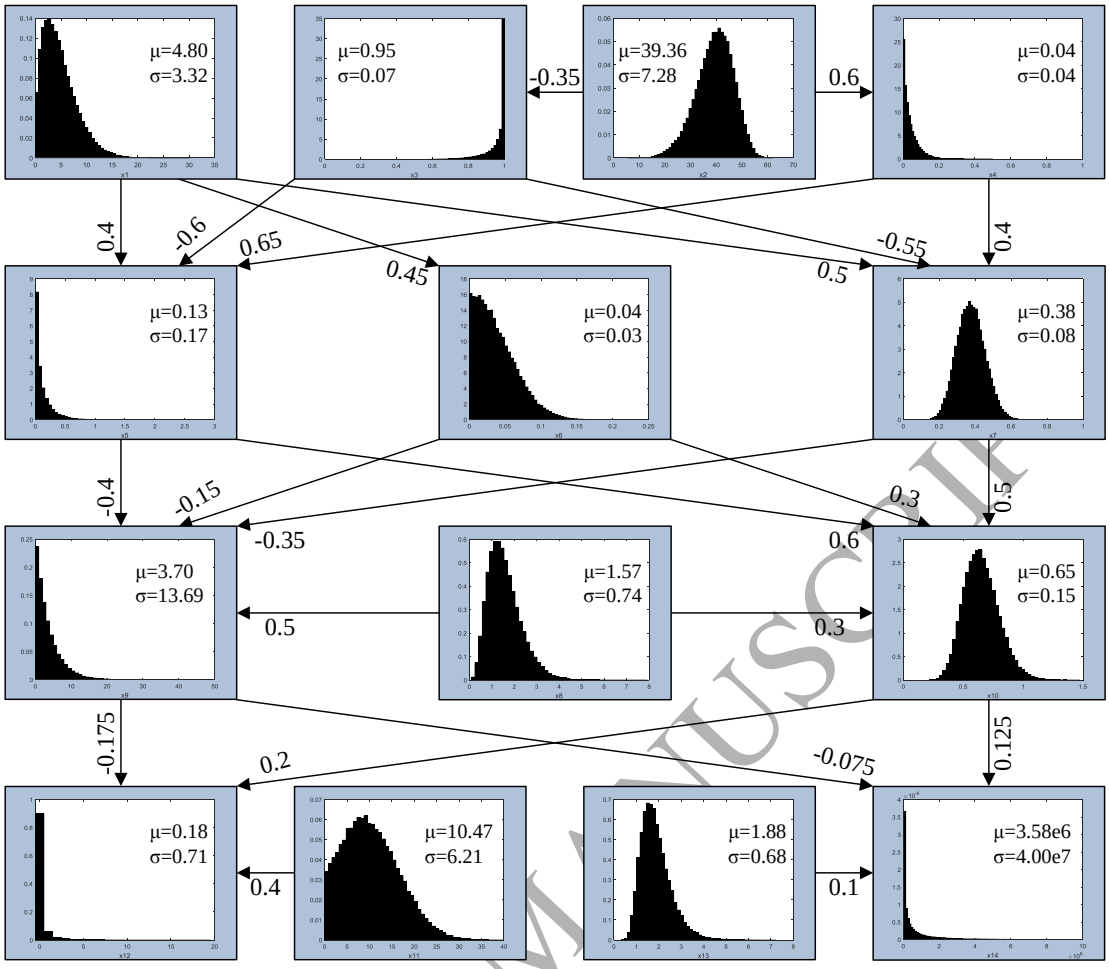

Fig. 10 Unconditional TBM tunneling risk model.

5.3 Model validation by documented accidents

The Fuxinglu-Lanjianglu twin tunnel (F-L tunnel, see Fig. 6) is a part of line 4 (Phase 2). Both lines were excavated using slurry shields. During the excavation of the last 150 m of the F-L tunnel, three accidents occurred. All accidents originated from a sudden water inflow. Preventive measures including dewatering, injection of polyurethane, and ground freezing were carried out after the detection of the inrush. It took approximately 10 hours on average to completely stop the water inflow. The accidents caused excessive deformation at the surface, and adjacent buildings were seriously damaged. Fig. 11 presents the damages incurred to the adjacent buildings. The estimate of total economic loss was approximately 2 million current CNY. Fortunately, the accidents did not result in injuries or deaths.

Fig. 11. Damages incurred to adjacent buildings.

Referring to the geological investigation report, the cover-span ratio of the last 150 m long tunnel was 2.75. The boreholes for geological investigation were drilled at an average interval of 44 m. According to the official report of the accident investigation, the main causes were: (1) the sandy soil strata contained a large amount of water under pressure while the soil above the tunnel crown was soft and instable; (2) the underestimation of the potential hazard related to the water bearing strata led to an inappropriate design and construction plan; (3) the incorrect position of the shield (the maximum tangent of pitching angle was 0.15) caused failure of the sealing system; (4) the poor emergency response and simplification of the shield receiving work plan also contributed to the accident occurrences.

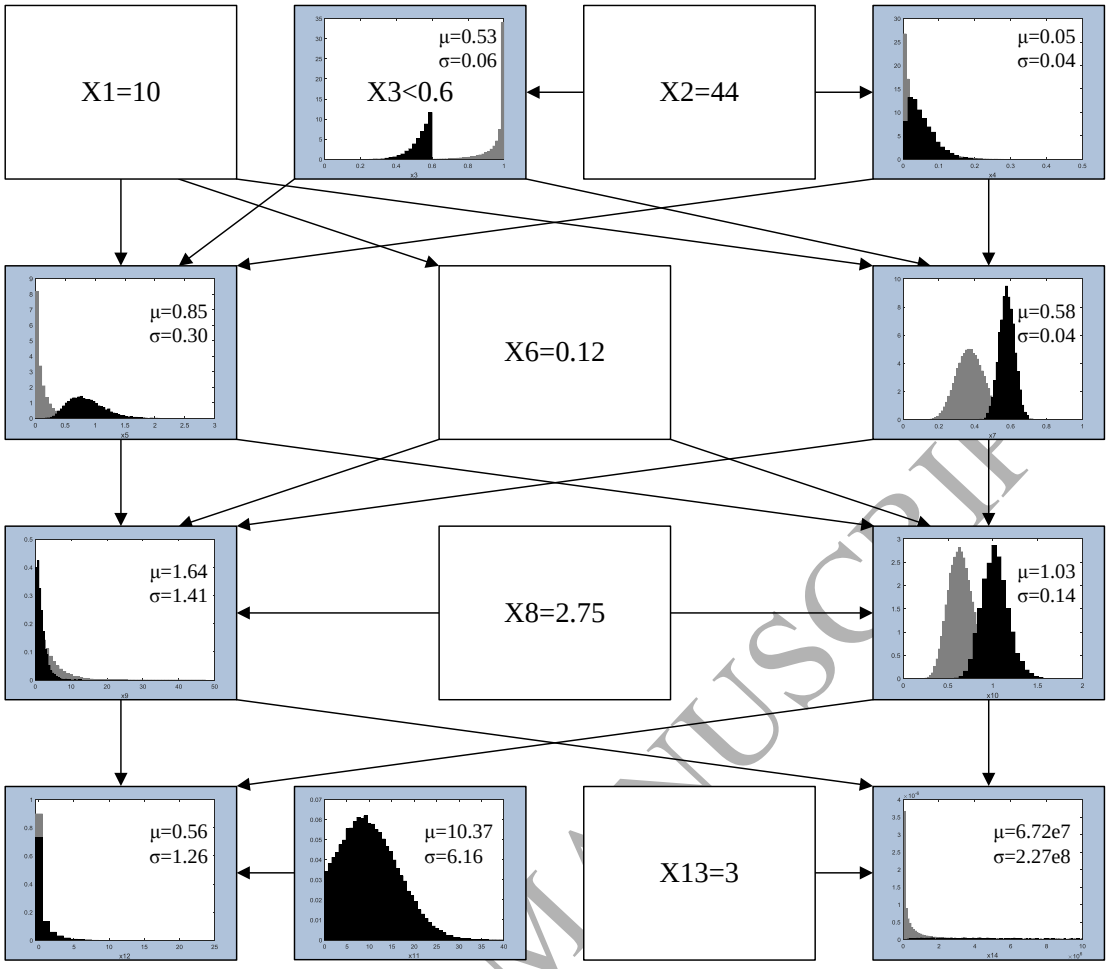

Fig. 12. Updated TBM tunneling risk model.

According to this evidence, the model could be updated by conditioning on the given observations. The average reaction time was fixed to 10 hours to represent a relatively poor management, while the analysis accuracy was set to be smaller than 60% due to the inappropriate design and construction plan. The average tangent of the pitching angle was 0.12, and the average floor ratio of the adjacent buildings was 3. Node X4 was not observed because the length of the water-bearing strata was not known. The updated model is given in Fig. 12. The histogram in gray represents the unconditional case for comparison. Fig. 13 presents the cobweb plot of the realizations of the random copula numbers. Because the mean value of the economic loss per 10 kilometers excavated increased to 6.72E7 CNY, the expected economic loss of the 300 m long excavation (both lines) was thus 189.8 million CNY, which is consistent with the real loss.

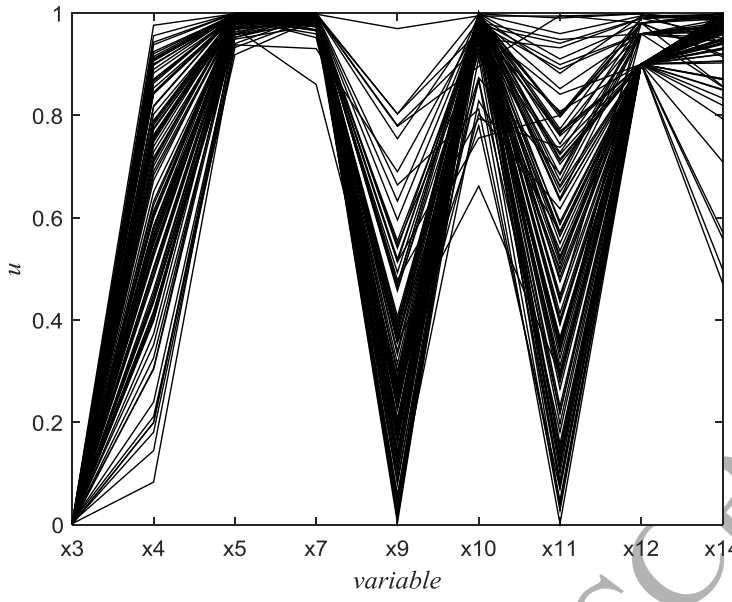

Fig. 13. Cobweb plot of the realizations of the random copula numbers.

5.4 Sensitivity analysis

A sensitivity analysis was conducted to identify the critical influencing factors with respect to the accident consequences. The hypothesis test for deviations between the unconditional and conditional mean was adopted [66]. The null hypothesis and alternative are defined as:

$$\begin{aligned} H_0 &: \mu^* = \mu \\ H_A &: \mu^* \neq \mu \end{aligned} \tag{23}$$

where μ^* is the mean of the conditional distribution given a certain event, while μ is the mean when no conditioning is made. Then, the statistic Z_H is formulated as:

$$Z_H = \frac{\mu^* - \mu}{\sigma / \sqrt{N}} \tag{24}$$

where σ is the standard deviation of the variable and N is the number of realizations of the event. A variable is considered to be sensitive to the event occurrence and thus important if the absolute value of Z_H is large.

We define two events, i.e., $EF_1 = \{X12 \geq 1\}$ and $EF_2 = \{X14 \geq 1e6\}$, to prioritize the importance of the remaining variables with respect to the number of fatalities and magnitude of the economic loss, respectively. Fig. 14 presents the

sensitivity analysis results. The sensitivities of the remaining variables to the two events are slightly different. For the risk of the loss of human life, the population density was considered the most important factor, followed by the accident frequency and magnitude. The surface occupation was correctly identified as the least important factor because it did not affect the number of fatalities. For the economic loss risk, the accident frequency and magnitude were ranked first and second, respectively, while the surface occupation was not among the top risk factors. The economic loss was not sensitive to the population density because they are independent. This difference reflects the difference in the expert knowledge on the loss of human life and the economic loss risk. When assessing the risk of the loss of human life, the major concern was the presence of third-party persons because the workers were protected by the TBM, whereas third-party persons were exposed to hazards and prone to be affected when an accident occurred. In contrast, some accidents only cause damage to the tunnels or TBMs. The economic loss can be substantial even if the adjacent buildings remain intact. Thus, the accident frequency and magnitude were the most important variables affecting the economic loss. The face instability and tail void ground loss were the two most important failure modes, which could be expected because most accidents were related to these two failure modes, while fewer accidents were caused by a poor boring orientation. Geological exploration was the most important among the four root causes because both the analysis accuracy and unknown geology depended on the geological investigation. The unpredicted adverse geological condition was also important because many accidents during tunneling are reported to have related factors, such as a high groundwater table or low soil stiffness.

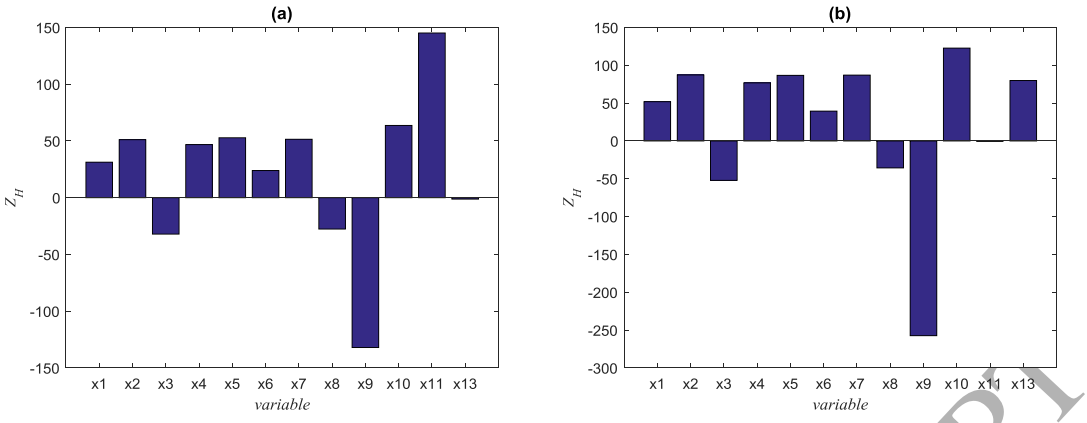

Fig. 14. Sensitivity of the variables with respect to (a) fatalities and (b) economic loss.

5.5 Discussion

The developed model can be used for other risk analysis purposes. For example, the contractor wants to determine the maximum reaction time according to the risk of loss of human life. Commonly, the number of fatalities is plotted against the frequencies (the F-N curve) to present this risk. Then the risk is classified as acceptable, unwanted, or unacceptable by comparing the F-N curve with given criterion. Decisions can then be made to ignore or reduce the risk [5]. Fig. 15 presents the F-N curves given several scenarios. The remaining variables remain unobserved. It is found that, if the risk is expected to maintain at the same level, the reaction time must be shorten from 12 hours to 2 hours when the population density increases from 10 persons per $100m^2$ to 15 persons per $100m^2$.

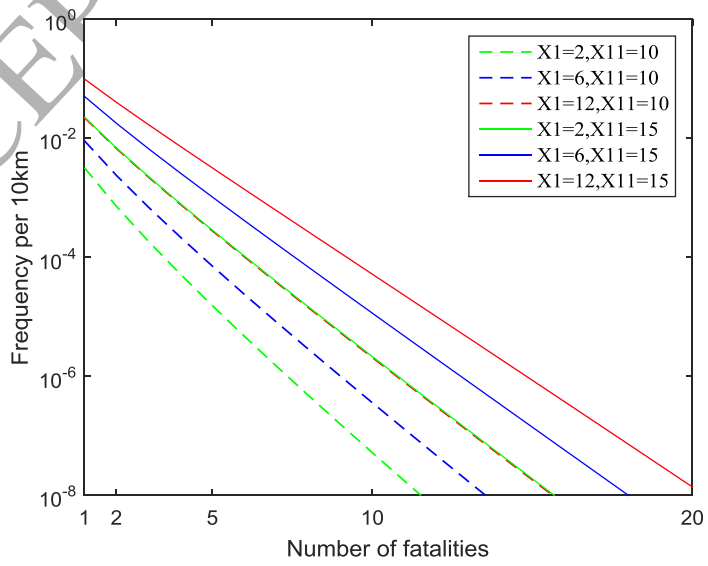

Fig. 15 F-N curves given reaction time and population density.

Moreover, the risk analysis result can be taken to guide the design of tunnels across cities. Fig. 16 demonstrates the economic loss risk corresponding to different tunnel cover-span ratios and average floor ratio of adjacent buildings. Generally, the risk increases as the average floor ratio increases or cover-span ratio decreases. However, it is found that the reduction in risk by increasing cover-span ratio is more significant when the surface occupational level is high. The risk contour suggests that the tunnel should be buried deeper when crossing densely populated regions and this design parameter can be determined quantitatively based on tolerant risks.

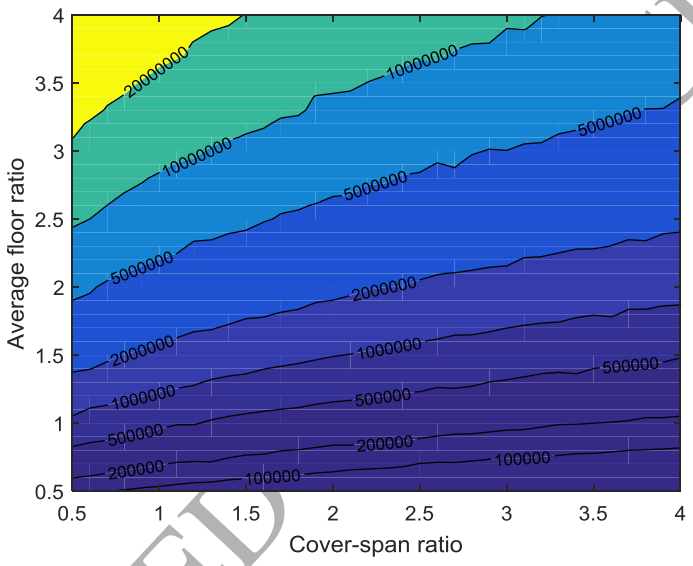

Fig. 16 Economic loss risk isolines given cover-span ratio and average floor ratio of adjacent buildings.

6 Conclusions

This study focuses on the development of knowledge-based expert systems for TBM tunneling risks. NPBN methodology is adopted due to its efficiency in modeling causal relationships. Because the risk assessment process resides mainly in the mind of the expert, expert judgments are elicited. In particular, the information on marginal distributions and pair-wise linear correlations are queried based on elicitation protocols. Then, the parametric univariate distribution is fitted to characterize the uncertainty of each node, while the copula parameter is determined to quantify the dependence associated with each edge.

The model for the Wuhan metro project risk analysis considers the root causes,

common failure modes, accident frequencies and magnitudes, and accident consequences. The discretization of the variables into states such as poor, fair, good is unnecessary, and all variables represented by nodes have natural number values. The invited experts are familiar and comfortable with the notion of Pearson's linear correlation. The proposed method can be extended to the use of Spearman's rank correlation by simply changing the marginals to a 0-1 uniform distribution. The elicitation process imposes less assessment burden on the experts considering the availability of experts.

The validated model can be used to assess risks due to TBM tunneling under different scenarios. The risk can be updated by conditioning on observations of the variables. Potential applications of the model, such as decision support for risk-based design, are also explored. Future studies should take more factors into account and refine the model for different purposes. For example, the focus on the face instability failure should include more shield parameters such as the penetration rate, degree of over-cutting or under-cutting, support pressure, and ground conditions such as the soil shear strength and pore pressure. However, the model refinement is not considered to be difficult because the NPBN is flexible and can incorporate more nodes. A model for other types of tunnels, such as NATM tunnels, can also be developed.

Acknowledgments

This work is supported by the National Natural Science Foundation of China (NSFC) under Grant No. 51608399.

References

[1] Einstein HH, Veneziano D. Risk analysis for tunneling projects: Massachusetts Institute of Technology; 2010.

[2] Landrin H, Blückert C, Perrin J, Stacey S, Stolfa A. ALOP/DSU coverage for tunnelling risks. Report No: IMIA WGP. 2006;48.

[3] Reilly J. Cost estimating and risk management for underground projects. Proc, International Tunneling Conference: Citeseer; 2005.

[4] Bravery P, Cross S, Gallagher R, Hautefeuille O, Reiner H, Spencer M, et al. A Code of Practice for Risk Management of Tunnel Works. Munich: The International Tunnelling Insurance Group. 2006.

[5] Eskesen SD, Tengborg P, Kampmann J, Veicherts TH. Guidelines for tunnelling risk management: international tunnelling association, working group No. 2. Tunnelling and Underground Space Technology. 2004;19:217-37.

[6] Wood AM. Tunnelling: management by design: CRC Press; 2002.

[7] Wearne S. Organisational lessons from failures. Proceedings of the Institution of Civil Engineers-Civil Engineering: Thomas Telford Ltd; 2008. p. 4-7.

[8] Mitchell JK. Geotechnical surprises-or are they? 1: the 2004 H. Bolton seed lecture. Journal of Geotechnical and Geoenvironmental Engineering. 2009;135:998-1010.

[9] Cárdenas IC, Al-jibouri SSH, Halman JIM, van Tol FA. Capturing and Integrating Knowledge for Managing Risks in Tunnel Works. Risk Analysis. 2013;33:92-108.

[10] Tserng HP, Yin SY, Dzeng R, Wou B, Tsai M, Chen W. A study of ontology-based risk management framework of construction projects through project life cycle. Automation in Construction. 2009;18:994-1008.

[11] Dong C, Wang F, Li H, Ding L, Luo H. Knowledge dynamics-integrated map as a blueprint for system development: Applications to safety risk management in Wuhan metro project. Automation in Construction. 2018;93:112-22.

[12] Tah J, Carr V. Knowledge-based approach to construction project risk management. Journal of computing in civil engineering. 2001;15:170-7.

[13] Choi H-H, Mahadevan S. Construction project risk assessment using existing database and project-specific information. Journal of Construction Engineering and Management. 2008;134:894-903.

[14] Dikmen I, Birgonul M, Anac C, Tah J, Aouad G. Learning from risks: A tool for post-project risk assessment. Automation in construction. 2008;18:42-50.

[15] Ayyub BM. Elicitation of expert opinions for uncertainty and risks: CRC press; 2001.

[16] Cárdenas IC, Al-Jibouri SS, Halman JI, van Tol FA. Modeling risk-related knowledge in tunneling projects. Risk analysis. 2014;34:323-39.

[17] Cooke RM, Goossens LH. Procedures guide for structural expert judgement in accident consequence modelling. Radiation Protection Dosimetry. 2000;90:303-9.

[18] Goossens LH, Cooke R, Hale AR, Rodić-Wiersma L. Fifteen years of expert judgement at TUDelft. Safety Science. 2008;46:234-44.

[19] Hallowell MR, Gambatese JA. Qualitative research: Application of the Delphi method to CEM research. Journal of construction engineering and management. 2009;136:99-107.

[20] Werner C, Bedford T, Cooke RM, Hanea AM, Morales-Nápoles O. Expert judgement for dependence in probabilistic modelling: a systematic literature review and future research directions. European Journal of Operational Research. 2017;258:801-19.

[21] Cárdenas IC, Al-Jibouri SS, Halman JI, van de Linde W, Kaalberg F. Using prior risk-related knowledge to support risk management decisions: lessons learnt from a tunneling project. Risk analysis. 2014;34:1923-43.

[22] Hong E-S, Lee I-M, Shin H-S, Nam S-W, Kong J-S. Quantitative risk evaluation based on event tree analysis technique: application to the design of shield TBM. Tunnelling and Underground Space Technology. 2009;24:269-77.

[23] Hyun K-C, Min S, Choi H, Park J, Lee I-M. Risk analysis using fault-tree analysis (FTA) and analytic

hierarchy process (AHP) applicable to shield TBM tunnels. Tunnelling and Underground Space Technology. 2015;49:121-9.

[24] Nývlt O, Prívara S, Ferkl L. Probabilistic risk assessment of highway tunnels. Tunnelling and Underground Space Technology. 2011;26:71-82.

[25] Qu X, Meng Q, Yuanita V, Wong YH. Design and implementation of a quantitative risk assessment software tool for Singapore road tunnels. Expert Systems with Applications. 2011;38:13827-34.

[26] Argenti F, Landucci G, Reniers G, Cozzani V. Vulnerability assessment of chemical facilities to intentional attacks based on Bayesian Network. Reliability Engineering & System Safety. 2018;169:515-30.

[27] Sýkora M, Marková J, Diamantidis D. Bayesian network application for the risk assessment of existing energy production units. Reliability Engineering & System Safety. 2018;169:312-20.

[28] Zhou Y, Li C, Zhou C, Luo H. Using Bayesian network for safety risk analysis of diaphragm wall deflection based on field data. Reliability Engineering & System Safety. 2018;180:152-67.

[29] Weber P, Medina-Oliva G, Simon C, Iung B. Overview on Bayesian networks applications for dependability, risk analysis and maintenance areas. Engineering Applications of Artificial Intelligence. 2012;25:671-82.

[30] Sousa RL, Einstein HH. Risk analysis during tunnel construction using Bayesian Networks: Porto Metro case study. Tunnelling and Underground Space Technology. 2012;27:86-100.

[31] Špačková O, Šejnoha J, Straub D. Probabilistic assessment of tunnel construction performance based on data. Tunnelling and Underground Space Technology. 2013;37:62-78.

[32] Špačková O, Straub D. Dynamic Bayesian network for probabilistic modeling of tunnel excavation processes. Computer‐Aided Civil and Infrastructure Engineering. 2013;28:1-21.

[33] Yu J, Zhong D, Ren B, Tong D, Hong K. Probabilistic Risk Analysis of Diversion Tunnel Construction Simulation. Computer‐Aided Civil and Infrastructure Engineering. 2017;32:748-71.

[34] Zhang L, Wu X, Skibniewski MJ, Zhong J, Lu Y. Bayesian-network-based safety risk analysis in construction projects. Reliability Engineering & System Safety. 2014;131:29-39.

[35] Wu X, Jiang Z, Zhang L, Skibniewski MJ, Zhong J. Dynamic risk analysis for adjacent buildings in tunneling environments: a Bayesian network based approach. Stochastic environmental research and risk assessment. 2015;29:1447-61.

[36] Zhang L, Wu X, Qin Y, Skibniewski MJ, Liu W. Towards a fuzzy Bayesian network based approach for safety risk analysis of tunnel‐induced pipeline damage. Risk Analysis. 2016;36:278-301.

[37] Wu X, Liu H, Zhang L, Skibniewski MJ, Deng Q, Teng J. A dynamic Bayesian network based approach to safety decision support in tunnel construction. Reliability Engineering & System Safety. 2015;134:157-68.

[38] Zhang L, Wu X, Ding L, Skibniewski MJ, Yan Y. Decision support analysis for safety control in complex project environments based on Bayesian Networks. Expert Systems with Applications. 2013;40:4273-82.

[39] Wang F, Ding L, Luo H, Love PE. Probabilistic risk assessment of tunneling-induced damage to existing properties. Expert Systems with Applications. 2014;41:951-61.

[40] Wang Z, Chen C. Fuzzy comprehensive Bayesian network-based safety risk assessment for metro construction projects. Tunnelling and Underground Space Technology. 2017;70:330-42.

[41] Sun J, Liu B, Chu Z, Chen L, Li X. Tunnel collapse risk assessment based on multistate fuzzy Bayesian networks. Quality and Reliability Engineering International. 2018:1-17.https://doi.org/0.1002/qre.2351.

[42] Neil M, Tailor M, Marquez D. Inference in hybrid Bayesian networks using dynamic discretization. Statistics and Computing. 2007;17:219-33.

[43] Langseth H, Nielsen TD, Rumí R, Salmerón A. Inference in hybrid Bayesian networks. Reliability Engineering & System Safety. 2009;94:1499-509.

[44] Hanea A, Napoles OM, Ababei D. Non-parametric Bayesian networks: Improving theory and reviewing applications. Reliability Engineering & System Safety. 2015;144:265-84.

[45] Hanea AM, Kurowicka D, Cooke RM. Hybrid method for quantifying and analyzing Bayesian belief nets. Quality and Reliability Engineering International. 2006;22:709-29.

[46] Nelsen RB. An introduction to copulas. New York: Springer; 2006.

[47] Morales-Nápoles O, Delgado-Hernández DJ, De-León-Escobedo D, Arteaga-Arcos JC. A continuous Bayesian network for earth dams' risk assessment: methodology and quantification. Structure and Infrastructure Engineering. 2014;10:589-603.

[48] Zilko AA, Kurowicka D, Goverde RM. Modeling railway disruption lengths with Copula Bayesian Networks. Transportation Research Part C: Emerging Technologies. 2016;68:350-68.

[49] Sebastian A, Dupuits E, Morales-Nápoles O. Applying a Bayesian network based on Gaussian copulas to model the hydraulic boundary conditions for hurricane flood risk analysis in a coastal watershed. Coastal Engineering. 2017;125:42-50.

[50] Lee D, Pan R. A nonparametric Bayesian network approach to assessing system reliability at early design stages. Reliability Engineering & System Safety. 2018;171:57-66.

[51] Morales O, Kurowicka D, Roelen A. Eliciting conditional and unconditional rank correlations from conditional probabilities. Reliability Engineering & System Safety. 2008;93:699-710.

[52] Clemen RT, Reilly T. Correlations and copulas for decision and risk analysis. Management Science. 1999;45:208-24.

[53] Clemen RT, Fischer GW, Winkler RL. Assessing dependence: Some experimental results. Management Science. 2000;46:1100-15.

[54] Bedford T, Cooke RM. Probability density decomposition for conditionally dependent random variables modeled by vines. Annals of Mathematics and Artificial intelligence. 2001;32:245-68.

[55] Bedford T, Cooke RM. Vines: A new graphical model for dependent random variables. Annals of Statistics. 2002:1031-68.

[56] Aas K, Czado C, Frigessi A, Bakken H. Pair-copula constructions of multiple dependence. Insurance: Mathematics and Economics. 2009;44:182-98.

[57] Joe H. Families of m-variate distributions with given margins and m (m-1)/2 bivariate dependence parameters. Lecture Notes-Monograph Series. 1996:120-41.

[58] Cooke RM, Goossens LL. TU Delft expert judgment data base. Reliability Engineering & System Safety. 2008;93:657-74.

[59] Delgado-Hernández D-J, Morales-Nápoles O, De-León-Escobedo D, Arteaga-Arcos J-C. A continuous Bayesian network for earth dams' risk assessment: An application. Structure and Infrastructure Engineering. 2014;10:225-38.

[60] Ross SM. Peirce's criterion for the elimination of suspect experimental data. Journal of engineering technology. 2003;20:38-41.

[61] Nápoles OM. Bayesian belief nets and vines in aviation safety and other applications. Unpublished Dissertation) Delft University of Technology, Delft, The Netherlands. 2010.

[62] Joe H, Li H, Nikoloulopoulos AK. Tail dependence functions and vine copulas. Journal of Multivariate Analysis. 2010;101:252-70.

[63] Lebrun R, Dutfoy A. An innovating analysis of the Nataf transformation from the copula viewpoint. Probabilistic Engineering Mechanics. 2009;24:312-20.
[64] Chua DK, Goh YM. Poisson Model of Construction Incident Occurrence. Journal of Construction Engineering and Management. 2005;131:715-22.
[65] Srb M. Possibilities of the collapse reduction during the excavation of conventional tunnels in the Czech republic. 2011.
[66] Walpole RE, Myers RH, Myers SL, Ye K. Probability and statistics for engineers and scientists: Pearson London; 2014.